Study of the Effect of Curve-Type Vortex Generator Pairs with Perforated and Flat Holes on Airfoil Performance

Saad Jabbar Nghaimesh

Mechanical Technology Department, Al-Nasiriyah Technical Institute, Southern Technical University, Al-Nasiriyah, Iraq, saad.nghaimesh@stu.edu.iq

In order to understand the processes of heat transfer, the investigation studies the flow and thermal properties of flat and curving generators with perforated sheets. The investigation conducts numerical simulations of the third dimension in a channel with two VGs located on the bottom of the wall, and varying the Re number from 3,000 to 27,500. The increase in heat transfer and pressure loss is quantified using the dimensionless parameters Num/Num0, f/f0, and R = (Num/Num0)/(f/f0). The results demonstrate that VGs with punched holes have a higher Num/ Num0 ratio than VGs without punched holes across all Re values, the greatest difference being observed at Re = 15,000. The coefficient of static friction (f/f0) initially increases rapidly, then reaches a steady state with Re, the highest of which is achieved by the RWP due to its larger area in comparison to the airflow in the P-series of VGs. Curved VGs CRW and CRWH have a greater effect on reducing drag and lowering the f/f0 of the device than flat VGs because of their streamlined configuration. The jet's flow from the perforations facilitates the clearance of still fluids and reduces the pressure differential between before and after the VGs. Also, the hydraulic heat capacity R is more beneficial in a curved VG than in a flat VG because of the enhanced heat transfer and lower wire consumption. The coefficient of thermal efficiency is determined by the combination of the Coulburn's and friction's coefficients, with CRWH having the greatest resistance. When Re is 9,000, a rectangularVG with holes has a higher performance than a counterpart that lacks holes, the maximum difference between the two is 33.2%.

Keywords: heat transfer, vortex generators, curved winglet.

1. Introduction

Heat transfer enhancement is of significant importance in such fields as power systems, the automobile industry, heating, ventilation, air conditioning systems aerospace, etc. However, as the heat transfer performance improves, the corresponding pressure drop also becomes tremendous for conventional passive methods such as adding fins or baffles. As is known that the air side thermal resistance is inherently higher than that on the liquid side for air e to e liquid and phase e change heat exchangers (HXs). A passive strategy for air-side heat transfer enhancement is to use longitudinal vortex generators (LVGs), which can be stamped

on or punched out from the surface of HXs. The earlier work using LVGs for heat transfer enhancement was reported by[1]. They found that the local Nu (Nusselt number) was increased at the position of LVGs while the overall Nu was not much increased due to the decrease elsewhere on the cylinder [2]. experimentally investigated the heat transfer enhancement and drag in transitional channel flow containing double rows of delta winglets. They reported that the critical angle of attack for the formation of longitudinal vortices behind the second row was smaller than that behind the first one, and the heat transfer coefficient and drag were increased by 80% and 160%, respectively.[3] compared several wing-type LVGs for heat transfer enhancement using the liquid crystal thermography method. They found the drag induced by LVGs was nearly proportional to the projected area and independent of Re and the shape of LVGs. [4, 5] studied the thermal and hydraulic characteristics of LVGs in the form of the delta wing, delta winglet pair, rectangular wing, and rectangular winglet pair in the rectangular channel flow. They quantitatively discussed the heat transfer enhancement mechanism in three ways: (1) developing boundary layers on the LVG surface; (2) swirling; and (3) flow destabilization. The following results were also presented: (1) winglets brought about higher heat transfer enhancement than wings for otherwise identical parameters; (2) the heat transfer enhancement was higher in laminar flow than that in turbulent flow; (3) for single vortex generators, heat transfer enhancement increased with the angle of attack and peaked at around 45. [6] studied the flow structures of LVGs in channel flow in numerical and experimental methods. They found the vortices were complex and consisted of a main vortex, a corner vortex, and induced vortices. The combined effect of these vortices distorted the temperature field in the channel and ultimately brought about the heat transfer enhancement between the fluid and its neighboring surface.[7] proposed a common flow-up configuration of winglets, which could augment heat transfer but reduce pressure loss in a fine tube heat exchanger. The results showed that heat transfer was increased by 10-30% and meanwhile, the pressure loss was reduced by 34-55% for a single row of winglets placed in a staggered arrangement compared with the situation without winglets. [8] studied the flow and heat transfer characteristics of a pair of embedded counter e rotating vortices using the thermos e chromatic liquid crystal method and they found that the common e flow e down cases showed better heat transfer characteristics than the common e flow e up cases. Different arrangements of LVGs to optimize the heat transfer enhancement and flow loss have been experimentally studied in Refs.[9] and the results showed that specially designed configuration could optimize the heat transfer coefficient. In addition to the study on configurations of LVGs, the development of new shape of LVGs attracts many researchers in recent years.[10] experimentally investigated the modified LVGs by cutting off the four corners of a rectangular wing and the heat transfer performance was reported to be improved.[11] proposed a kind of LVG called curved trapezoidal winglet and experimentally investigated its performance of heat transfer enhancement and flow resistance by comparison with those of traditional vortex generators e rectangular winglet, trapezoidal winglet, and delta winglet. The results indicated that curved trapezoidal winglet pairs performed better in fully turbulent regions with higher heat transfer enhancement and lower pressure loss.[12] studied the heat transfer enhancement of punched LVGs using the infrared thermal image technique. He reported a 23-55% increase in heat transfer performance and correlations for Nu were developed for corresponding LVGs[13] numerically studied the hydrodynamic performances from a rectangular channel fitted with

LVGs and found the heat and mass transfer were intensified for a transient estate flow. [14] investigated four horizontally placed plates with a pair of delta winglets punched directly from the plates at an attack angle of 15, 30, 45, and 60, respectively. The results revealed that the average Nu on the plate increased with the increase of attack angle. [15] numerically studied the flow structure and heat transfer enhancement of LVGs applied in direct air-cooled condenser using the RNG k-ε model and found that the delta winglet pair with an attack angle of 25 could reach the optimum thermal and flow performances fitted curved rectangular vortex generators in the wake regions of a fine tube exchanger and found that the heat transfer performance was significantly improved.[16] The inherent mechanism of heat transfer enhancement by LVGs can be explained in two folds from the above literature: (1) the secondary flow induced by LVGs swirls and disturbs the fluid flow; (2) the boundary layer is distorted and thinned, which is mainly from the point of qualitative description. The previous literature used VGs that were punched directly from the plat or wavy fins, resulting in holes located in front of the VGs. However, the holes on the surface fins have minimal impact on reducing form drag in the recirculation zone, where the normal-wise velocity is small. To improve heat transfer performance and reduce pressure loss in the recirculation zone, Zhou et al. proposed punching holes on the surfaces of the VGs. This allows fluid to be ejected through the holes, taking stagnant fluids to the main flow. The effects of hole size and position were evaluated using dimensionless factors, and it was found that flow resistance was reduced and heat transfer was improved. However, the mechanism behind how the holes enhance heat transfer and reduce pressure loss needs further study, and the position and diameter of the holes should be optimized for different types of VGs. The field synergy principle (FSP) and secondary flow theory are adopted in this paper to clarify the mechanism of heat transfer augmentation and pressure loss of VGs with and without punched holes. Additionally, the diameter and position of the holes punched from the surface of VGs are optimized.

2. Physical and mathematical model

2.1. Physical model

Three-dimensional numerical simulations are carried out in a rectangular air channel where several kinds of winglet pairs are fastened to the lower wall. The winglets consist of, CRWP, CRWH, RWP, and RWH. These winglets have holes drilled in them at various locations. The winglets and holes' measurements and ratios are given. Figures demonstrate how the computational domain and winglets are configured. A coordinate system in Cartesian space is used to characterize the flow. Figure 1(a) depicts the LVG configurations, and Table 1 gives the geometric characteristics. Figure. 1(b) depicts the air channel size with a winglet pair. The flow is given in a Cartesian coordinate system (x, y, z), where x, y, z denotes streamwise, spanwise, and wall-normal directions. The channel is 1000 mm x 240 mm x 40 mm (L x W x H). At a 45-degree attack angle, a pair of LVGs are positioned in a shared flow-down configuration. The winglet pair is located 170 mm downstream of the channel intake and has a transverse gap of 10 mm between the leading edges. According to an experimental study by [17]

Table 1 Geometric parameters of vortex generators.

Type	α	β(°)	a(mm)	b(mm)	h(mm)	S(mm)	φ
RWP	/	45	50	0	30	25	/
CRWP	20	45	50	10	30	25	/
RWH	/	45	50	0	30	25	0,0.04,0.08,0.09,0.13
CRWH	20	45	50	10	30	25	0,0.04,0.08,0.09,0.13

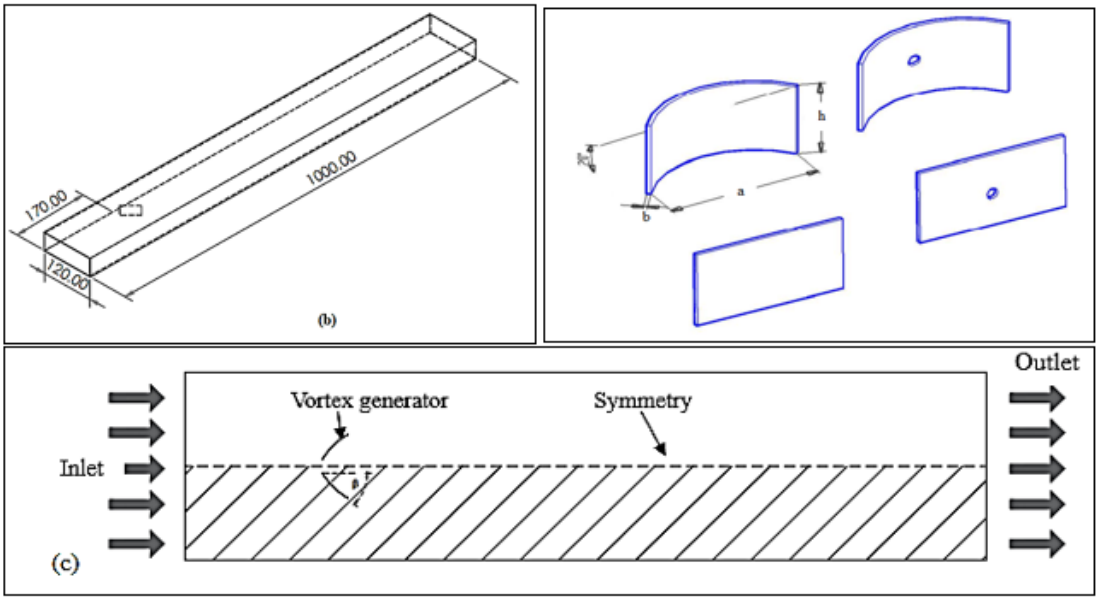

Fig.1.Physical model: (a) Vortex generator; (b) Channel geometry and Pair of vortex generators; (c) Model calculation range taking CRWP as an example

2.2 Boundary conditions

The computational domain diagram is proven in Figure 1(c). Rigid partitions consist of square walls and VGs, which might be defined as non-slip boundary conditions. For the inlet boundary condition, the air pace and temperature are assumed to be uniform, u = u in, v = w = 0, T = Tin, and the strain pin is atmospheric stress. For the main phase of the channel, the surface temperature at the lowest wall is regular, and the last partitions are assumed to be adiabatic,$x = \partial T/\partial y = \partial T/\partial Z = 0$. For the prolonged segment, all walls are assumed to be adiabatic. The symmetry wall applies a symmetry boundary circumstance, v = 0,$\partial u/\partial y = \partial w/\partial y = 0, \partial T/\partial y = 0$. The output is about a fully advanced boundary circumstance, $\partial u/\partial x = \partial v/\partial x = \partial w/\partial x = \partial T/\partial z = 0$.

2.3 Governing equations

These assumptions lead to the following written equations.

Continuity equation:

$$\partial uj/\partial xj = 0, \quad j=1,2,3 \tag{1}$$

Momentum equation for turbulent flow:

$$\frac{\partial ujui}{\partial xj} = \frac{\partial p}{\partial xj} + \frac{\partial}{\partial xj}\left(u\frac{\partial ui}{\partial xj} - \rho uj^{-}ui^{-}\right), (i,j = 1,2,3; i \neq j) \tag{2}$$

Energy equation: $\rho cp\ uj\ (\partial T/\partial xj) = \partial y/\partial x\ (\lambda\ \partial T/\partial xj), (j = 1,2,3)$ (3)

In this study, the use of the SST k-ω model necessitates an assessment of the wall adjacent cell size analogous to the dimensionless wall distance y^+ less than 4, ensuring that the viscous sublayer is meshed [18]. The SST k-ω model transport equations.

$$\rho\frac{\partial}{\partial x_i}(ku_i) = \frac{\partial}{\partial x_j}\left(\Gamma_k\frac{\partial k}{\partial x_j}\right) + \tilde{G_K} - Y_K \tag{4}$$

$$\rho\frac{\partial}{\partial x_i}(\omega u_i) = \frac{\partial}{\partial x_j}\left(\Gamma_\omega\frac{\partial \omega}{\partial x_j}\right) + G_\omega - Y_\omega + D_\omega \tag{5}$$

Where:

$\tilde{G_k}$, Production of turbulence kinetic energy due to mean velocity gradients, G_ω, Generation of ω,

Γ_k, Effective diffusivity of k; $(\Gamma_k = \mu + \frac{u_i}{\partial_k})$; Γ_ω, Effective diffusivity of ω; $(\Gamma_\omega = \mu + \frac{u_i}{\partial_\omega})$; Y_K Dissipation of k due to turbulence, Y_ω Dissipation of ω due to turbulence, D_ω Cross-diffusion, ∂_K, ∂_ω turbulent Prandtl number for K and ω respectively, and μ_t Turbulent viscosity.

The boundary condition at the inlet, velocity is fully devolved.

$$T_{in} = 300\ K \text{ at } x = 0, \frac{\partial u}{\partial z} = \frac{\partial u}{\partial y} = 0, w = v = 0 \tag{6}$$

$$\frac{dT_f}{dx} = 0, \frac{\partial u}{\partial x} = \frac{\partial v}{\partial y} = \frac{\partial w}{\partial z} \tag{7}$$

$$u = w = v = 0 \tag{8}$$

At the top surface, a uniform temperature is applied as

$$T = T_s = 350[K] \tag{9}$$

Bottom and side walls are considered adiabatic walls

$$\left.\frac{\partial T}{\partial z}\right|_{z=H} = 0, \left.\frac{\partial T}{\partial z}\right|_{y=0} = 0 \tag{10}$$

The conjugate heat transfer between LVG surfaces (solid) and fluid

$$T_s = T_f \quad \text{And} \quad k_s\left(\frac{\partial T}{\partial n}\right)\Big|_f = k_s\left(\frac{\partial T}{\partial n}\right)\Big|_s \tag{11}$$

Where n is a normal vector on longitudinal vortices generator drawn outward the boundary.

The boundary condition for the symmetry plane can be written as.

$$\frac{\partial T}{\partial x} = \frac{\partial T_s}{\partial x} = 0 \ , \ u = 0 \tag{12}$$

2.4 Solution method

The mathematical model of air channels with LVGs is solved using the FLUENT - 16.2 CFD program. Laminar and RNG k-ε models are applied for laminar and turbulent flow respectively. Enhanced wall function is used for accurate heat transfer modeling in near-wall regions for turbulent flow. The finite volume method and SIMPLE algorithm are used for solving governing equations for both models. The second-order upwind scheme is used for convective terms and the central difference scheme is used for diffusive terms in momentum and energy equations. Residuals of 10-5, 10-6, and 10-7 are used to verify the convergence of continuity, momentum, and energy equations respectively. Under-relaxation factors for momentum and pressure are set to 0.4 and 0.8 respectively for the current computation.

2.5. Parameter characterization

To present the simulation results, the following parameters are defined:

$$\mathrm{Re} = \frac{\rho V_{in} D_h}{\mu} \tag{13}$$

$$D_h = \frac{2W.H}{W + H} \tag{14}$$

$$Nu = \frac{hD_h}{k} \tag{15}$$

$$Q = \dot{m} c_p (T_{out} - T_{in}) \tag{16}$$

$$\eta = (\frac{Nu}{Nu_{bf}})(\frac{f_{bf}}{f})^{\frac{1}{3}} \tag{17}$$

$$h = \frac{Q}{T_{wall} - (\frac{T_{in} + T_{out}}{2})} \tag{18}$$

$$f = \frac{2\Delta p}{\rho V_{in}^{\ 2}} \times \frac{D_h}{L} \tag{19}$$

$$\Delta p = (p_{in} - p_{out}) \tag{20}$$

$$Pr = \frac{c_p \mu}{k} \qquad (21)$$

3. Grid independence and model validation

The 3-D grid system for all the fluid domains is divided into several sub-domains and different strategies are employed for different sub-domains to generate the mesh. The region around the LVGs (60 mm X 120 mm X 40 mm) meshes using unstructured tetrahedral elements with further refined grids to deal with the flow separation and secondary flows. For the rest channel domains, a structured hexahedral grid is used for its simple physical model. Grid independence tests are carried out in the following method before further numerical work. Six sets of grid numbers, i.e. 22 X 104, 24 X 104, 36 X 104, 48 X 104, 86 X 104, and 95 X 104, are adopted to examine the influence of the grid number on the calculation with CRWP. It can be seen that the discrepancy of Num for grid numbers 86 X 104 and 95 X 104 is 1.8%, and then grid number 86 X 104 is applied in simulation to keep a moderate accuracy while saving computation time.

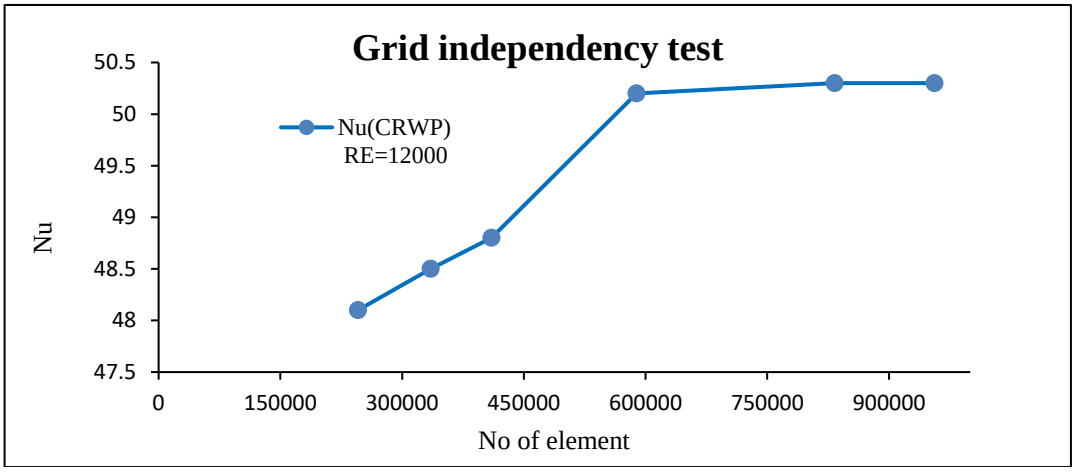

Fig. 2. Grid independence verification for CRWH (Re = 12,000)

The simulated results for channel flow with and without LVG pairs were compared with empirical correlations and experimental data. As shown in Fig. 3, the Num of the smooth channel (without LVGs) is in reasonable agreement with the Hausen correlation in the laminar region and the Gnielinski correlation for turbulent flow with a maximum difference of 7.1%. Similarly, the calculated friction factors of the smooth channel agree well with Poiseuille's law in laminar flow and Blasius correlation in turbulent regions with a maximum difference of 6.3%. The above correlations are cited from [19] and are listed here.

Hausen correlation:

$$\mathrm{N_{um}} = 3.66 + \frac{0.668(\mathrm{D/L}) * \mathrm{RePr}}{1 + 0.04[(\mathrm{D/L})\,\mathrm{RePr}]^{2/3}} \qquad (22)$$

Gnielinski correlation:

$$N_{um} = 0.0214(Re^{0.8} - 100)\, Pr^{0.4} \quad (23)$$

Poiseuille's law:

$$f = 64/Re \quad (24)$$

Blasius correlation:

$$f = 0.3164 Re^{-0.25} \quad (25)$$

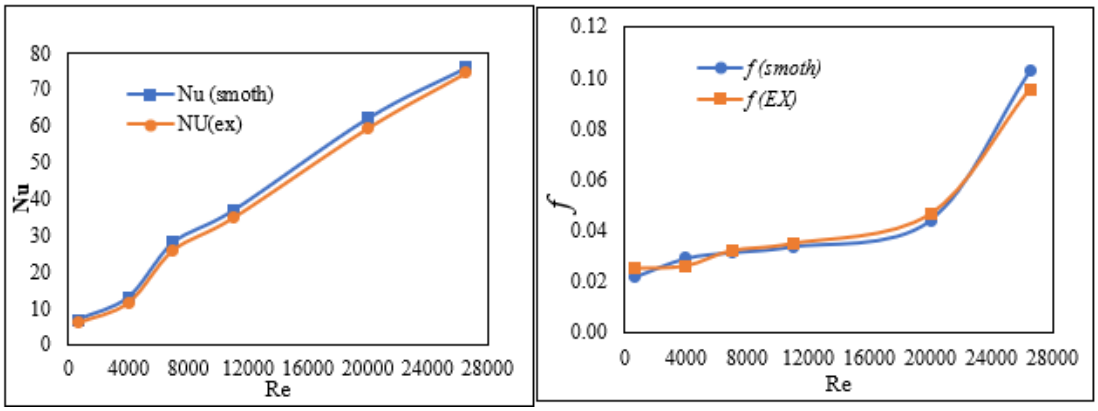

Fig. 3. Comparison of (Num) and (f) between numerical results and experimental relationship

4. Results and discussions

4.1. Comparison of heat transfer enhancement and flow loss among different LVGs

In this section, the heat transfer and flow loss performances of different vortex generators are discussed, and R = (Num/Num0)/ (f/ f0) is used to evaluate the overall performance. Figure 4 shows the normalized average Nusselt number, Num/Num0 (Num0 is the average Nusselt number for the smooth channel without LVGs). It is found that the Num/Num0 of level VGs with (CRHW) is slightly higher than the rest of the levels corresponding to all Re and that the deviation of Num/Num0 between CRWP and RWHP and RWP reaches 3.5% at Re = 3000. RWP is also present in the highest Num/Num0 range between 1.23 and 1.45, followed by CWP and RWP respectively. This is because the RWP has the largest area facing the airflow, resulting in the strongest longitudinal vortices. The same trend is also found for the corresponding curved vortex generators. For each LVG, Num/Num0 first increases with Re reaches its peak in the transition region and then decreases in the disordered region.

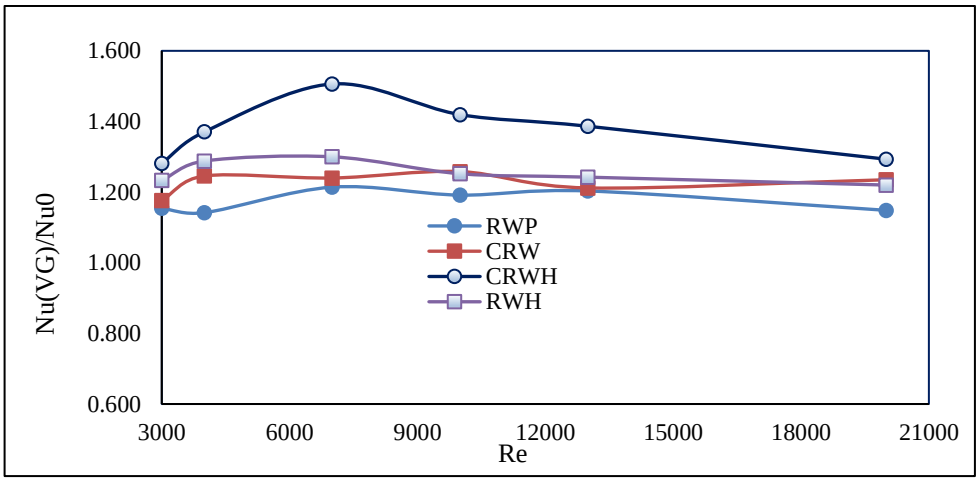

Fig. 4. Comparison of the performance of six types of LEGs at different Reynolds numbers with Num/Num0

The pressure drop is expressed in terms of apparent friction factor f/f0. It is found in Fig. 5, that f/f0 first increases sharply and then becomes stable with Re. For the P-series of VGs, the friction factor f/f0 of CRHWP is the highest ranging from 1.6 and 2.1 followed by CRWP and RWP and RWHP successively due to the abovementioned largest area facing the air flow. Moreover, the H-series of VGs show lower pressure loss than P-series VGs over the Re investigated. This is because the jet flow from the holes can remove the stagnant fluids and diminish the pressure difference before and after the VGs.

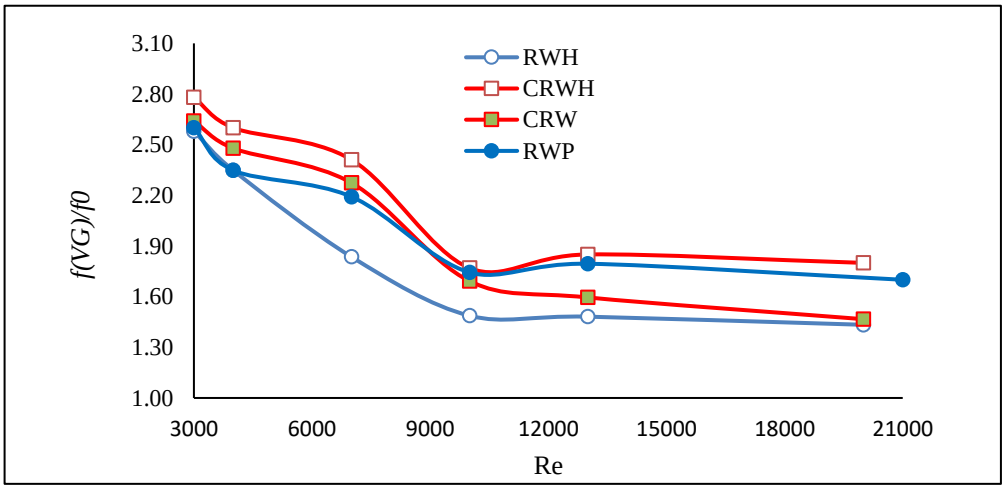

Fig. 5. Comparison of the performance of six types of LEGs at different Reynolds numbers with f/f0

The thermo-hydraulic performance R covering all the flow regions of all these VGs is shown in Fig. 6. It can be seen that with the increase of Re, the value of R decreases. For the same shape of VGs, the H-series perform better than the P-series and the curved VGs perform better than the corresponding plane VGs due to the combined effect of heat transfer

enhancement and flow floss reduction.

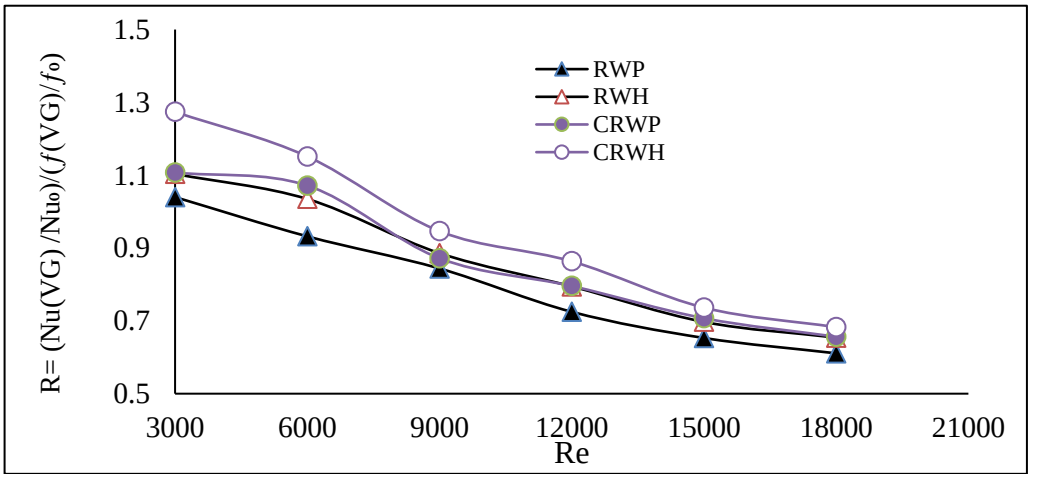

Fig. 6. Comparison of performances of plane and curved VGs with and without holes (Num/Num0)/(f/f0) vs. Re

Impact of different sizes of perforated holes on the effectiveness of VG

Additional simulations were conducted to assess the impact of hole diameter on the flow and heat transfer properties of VGs. It is important to note that the holes are punched in the center of these VGs, with l'/a = 1/2 and h''/h'= 1/2. As shown in Fig. 7(a), the Num/Num0 initially increases and then sharply declines with the increase in the hole area. A hole area ratio of φ = 0.06 provides the best heat transfer enhancement, with Num/Num0 reaching as high as 1.18 to 1.39. However, for φ = 0.09 and 0.13, poorer heat transfer enhancement is observed compared to VGs without holes, which is consistent with the findings of experiments conducted by [17]. This is attributed to the fact that the jet from the holes can reduce the wake region and improve heat transfer, but it also diminishes the pressure difference before and after the VGs, leading to a decrease in the strength of longitudinal vortices and a subsequent reduction in heat transfer enhancement. With larger holes, this negative effect may become more pronounced and worsen the heat transfer enhancement.

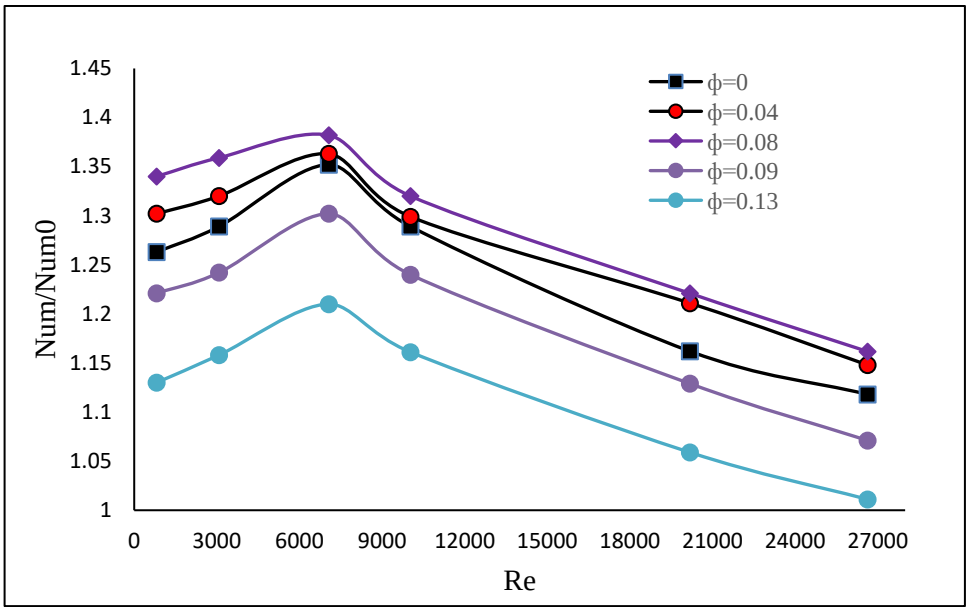

Fig. 7. Impact of the size of the hole for RWH: (a) Num/Num0 vs. Re

Figure 7(b) illustrates how the diameter of holes affects pressure loss. The results show that creating holes on VGs can effectively reduce flow resistance across the entire range of Reynolds numbers studied. Additionally, the larger the hole area, the lower the flow resistance due to decreased form drag. For the largest hole examined in this study (with a diameter of φ=0.13), the pressure loss was reduced by 12–14%.

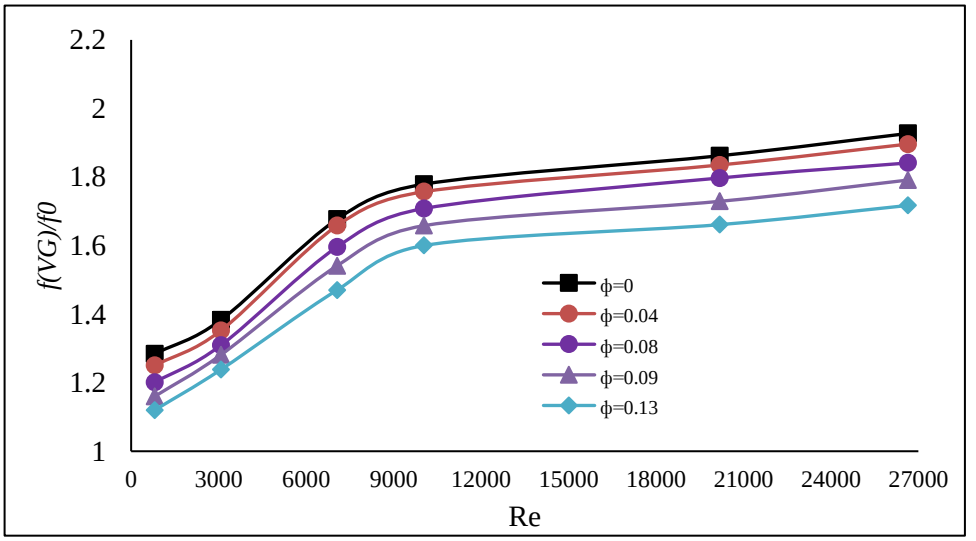

Fig. 7. Impact of the size of the hole for RWH: (b) (f(VG)/f0) vs. Re

4.3. Impact of hole punching position on the performance of VG

The position of the holes through which the jet enters the fluid outside the VG greatly

influences the heat transfer and pressure loss, as shown in Figure 8. As can be seen in Figure 8 (a), hole drilling position at a lower length punching hole at high for the same l'/a = 1/2 Comparatively results in better heat transfer efficiency. Drilling holes at a higher elevation may disturb and weaken the main elliptical vortex formed in the downstream stream, thereby affecting the heat transfer efficiency. On the other hand, drilling holes at a lower altitude can cause the low-velocity zone to recirculate behind the wall, with little effect on the surface vortex, increasing the local heat transfer besides, holes drilled near the face are found to have better thermal performance than the adjacent holes at the same height. The reason is that the jet near the front will hit most of the stability zone outside the VG as shown in Fig. 8(b) which highlights the effect of the pore location on the flow resistance. This indicates that in cases of uniform pore area, the position of the pore slightly influences the pressure loss because the form drag is mainly related to the VGs' frontal face area, in good agreement with the experimental results of [17].

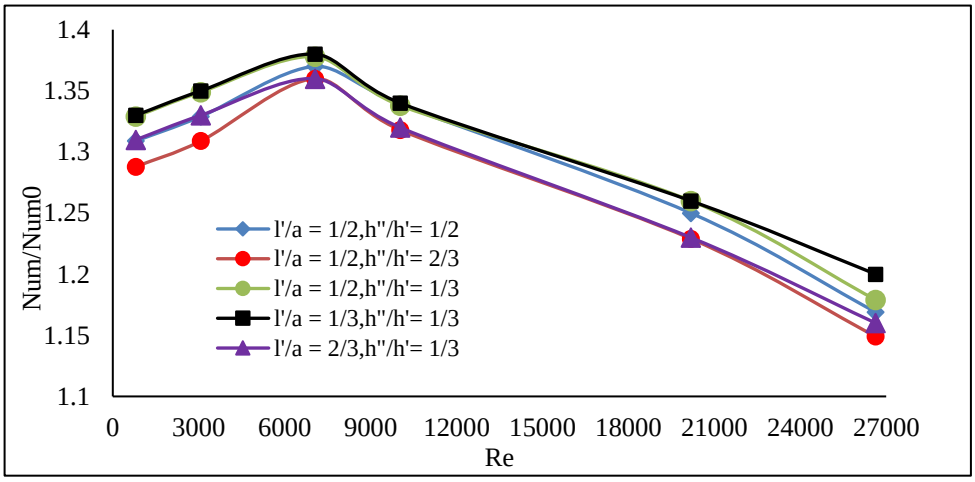

Fig. 8. The impact of the puncture location on TWH(a) Num/Num0 vs. Re

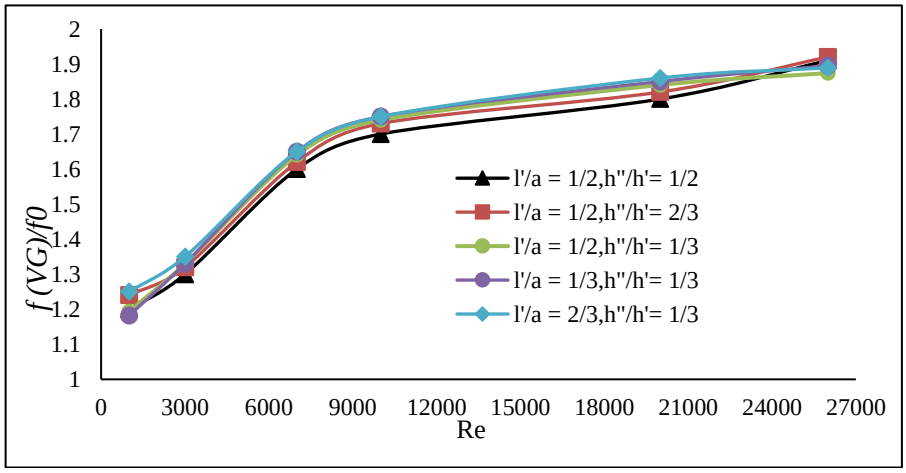

Fig. 8. The impact of the puncture location on TWH(b) (f(VG)/f0) vs. Re

4.4. The system's thermal efficiency

PEC decreases with increasing Reynolds number. While the PEC values of the vortex generators in the laminar region are similar, the difference becomes more pronounced in the turbulent region. Vortex generators with curved geometries and holes have higher PEC compared to those without them, especially at lower Reynolds numbers. The thermal-hydraulic efficiency coefficient includes the Colburn and friction coefficients, with CRWH having the highest resistance, followed by CRWP, RWP, and RWH. At Re = 9,000, the performance of the curved VG with holes is 33.2% better than that without.

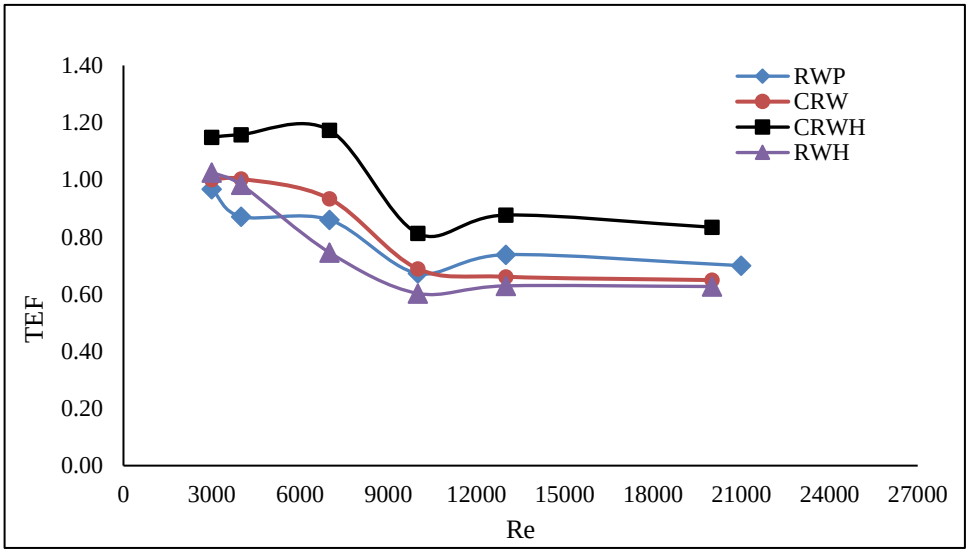

Fig. 9. displays the numerical simulation results for TEF with a channel that features curved VGs.

4.5. Temperature and velocity contour

The text describes temperature variations and flows in a channel with multiple long-term vortex generators (LVGs). Initially, a weak temperature gradient occurs along the width of the channel due to the near equality of the flow and adiabatic conditions near the wall Low flows alternating LVGs occur, giving rise to central jets and eddies. Five distinct regions appear along the extension, where the strong downward temperature near the central jet axis and the wake behind the LVGs promote mixing and heating the size of the separation bubble increases with velocity the penetration rate increases. The second LVG pair exhibits strong mixing and heating due to convection and weak effects of the central jet The temperature rise at the surface layer is moderated by mixing for increasing concentration, and the fracture jump was stronger with increasing Reynolds number (Re).

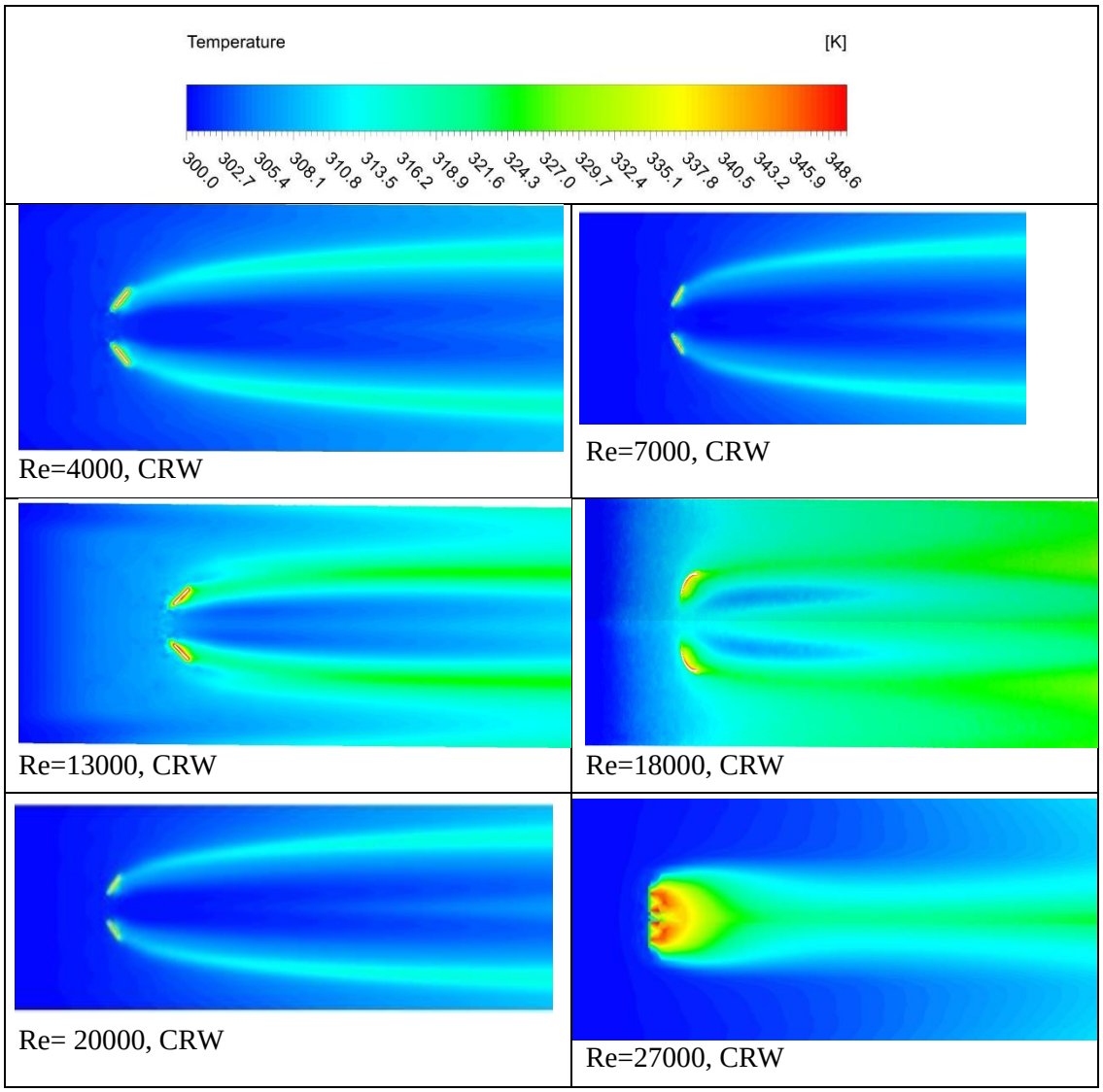

Fig. 9. Temperature contour.

The text discusses computational fluid dynamics (CFD) analysis of flow around two wings. The maximum velocity values occur on the two wings, after which different velocity regions are observed due to the longitudinal vortex Similar features are observed near the symmetric axis, corresponding to induced vortices. Experimental and numerical results agree well, showing symmetric topologies in the mean transverse velocity components. The breakup of the flow behind the two birds causes water to flow down between them, creating two main elliptical vortices separated by the y/H=0 axis Two clockwise and counterclockwise vortices develop, with good agreement between experimental and numerical data. However, differences in the generation of the second vortex are noted, especially above x/H=3, indicating limitations in the SST turbulence model.

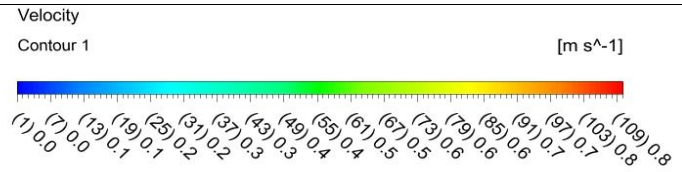

Re=4000, CRW

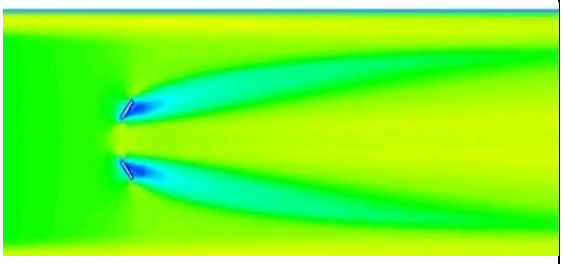

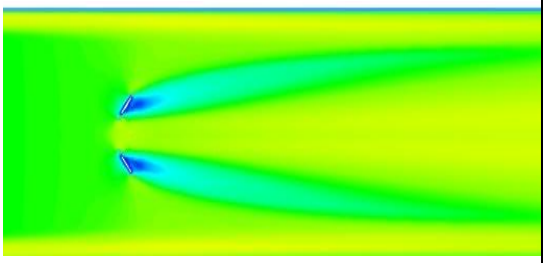

Re=7000, CRW

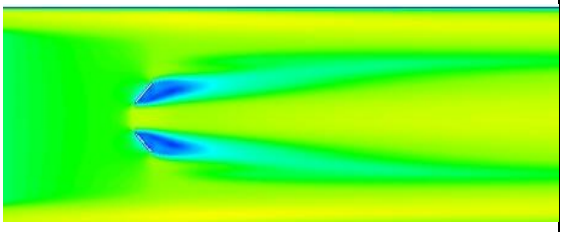

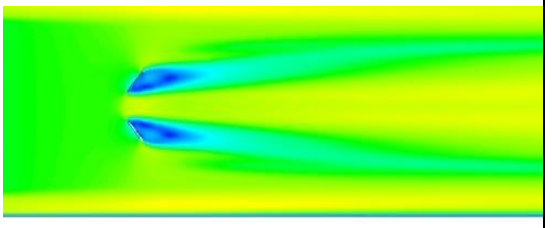

Re=18000, CRW

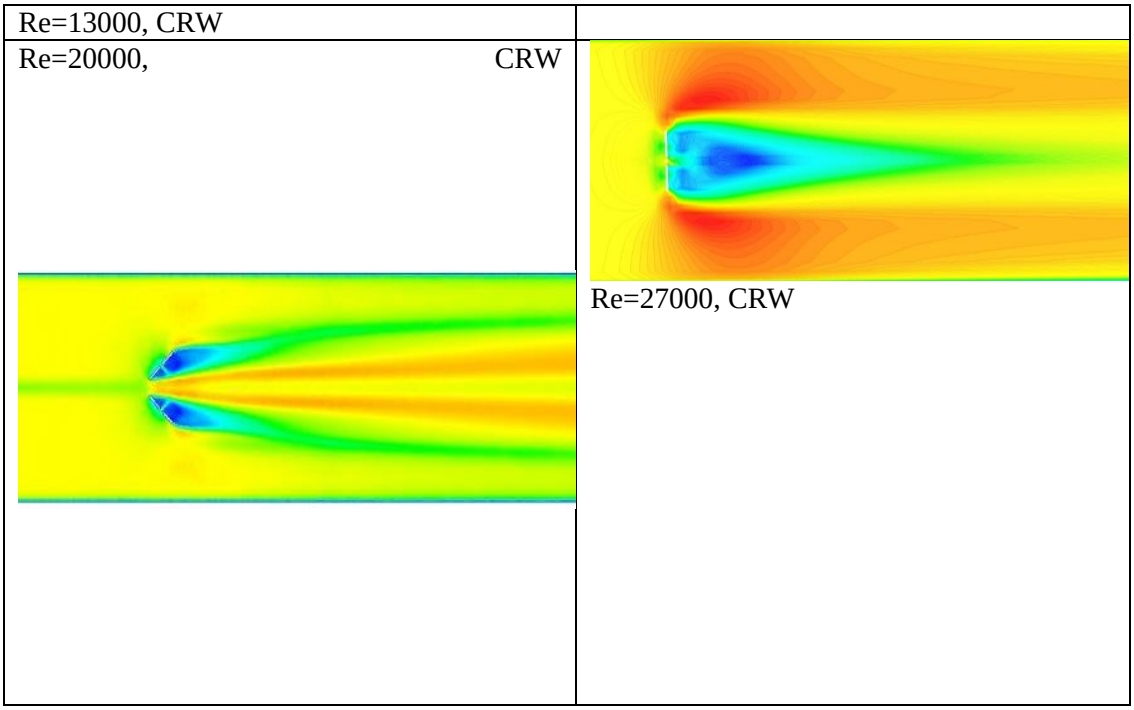

Fig .11. velocity contour

5. Conclusions

The present study involves conducting 3-D numerical simulations in a channel flow with various VGs attached to the bottom wall. The analysis focuses on the heat transfer performance and flow resistance of the VGs. The results are interpreted based on secondary flow theory and field synergy principle. The key findings can be summarized as follows, Creating perforations on the surface of vortex generators (VGs) can enhance heat transfer and reduce flow resistance. When comparing curved VGs to plane VGs under the same conditions, the former showed a 9.3–16.9% improvement in overall performance due to their streamlined design. Analysis of secondary velocity vectors and streamlines revealed that a higher Nusselt number (Nu) is closely related to better coordination between the velocity vector and temperature gradient, and the fluid-structure parameter (FSP) can explain the mechanism of heat transfer enhancement. It is important to match the area of punched holes with the VG area to achieve optimal heat transfer enhancement. The best ratio of hole area to VG area is 0.06 under the current conditions, resulting in a higher R value (0.65–1.18) compared to corresponding VGs without holes (R-value: 0.57–0.95). Punching holes at a lower position in the vertical direction and close to the leading edge of the VGs improves heat transfer enhancement, while the position of the holes has minimal impact on flow resistance.

References

1. Johnson, T.R. and P.N. Joubert, The influence of vortex generators on the drag and heat transfer from a circular cylinder normal to an airstream. 1969.
2. Tiggelbeck, S., N. Mitra, and M. Fiebig, Comparison of wing-type vortex generators for heat transfer enhancement in channel flows. 1994.
3. Biswas, G., H. Chattopadhyay, and A. Sinha, Augmentation of heat transfer by creation of streamwise longitudinal vortices using vortex generators. Heat Transfer Engineering, 2012. 33(4-5): p. 406-424.
4. Fiebig, M., Embedded vortices in internal flow: heat transfer and pressure loss enhancement. International Journal of Heat and Fluid Flow, 1995. 16(5): p. 376-388.
5. Fiebig, M., Vortices, generators and heat transfer. Chemical Engineering Research and Design, 1998. 76(2): p. 108-123.
6. Biswas, G., et al., Numerical and experimental determination of flow structure and heat transfer effects of longitudinal vortices in a channel flow. International Journal of Heat and Mass Transfer, 1996. 39(16): p. 3441-3451.
7. Kwak, K., K. Torii, and K. Nishino, Simultaneous heat transfer enhancement and pressure loss reduction for finned-tube bundles with the first or two transverse rows of built-in winglets. Experimental Thermal and Fluid Science, 2005. 29(5): p. 625-632.
8. Skullong, S. and P. Promvonge, Experimental investigation on turbulent convection in solar air heater channel fitted with delta winglet vortex generator. Chinese Journal of Chemical Engineering, 2014. 22(1): p. 1-10.
9. Khoshvaght-Aliabadi, M., O. Sartipzadeh, and A. Alizadeh, An experimental study on vortex-generator insert with different arrangements of delta-winglets. Energy, 2015. 82: p. 629-639.
10. Min, C., et al., Numerical investigation of turbulent flow and heat transfer in a channel with novel longitudinal vortex generators. International Journal of Heat and Mass Transfer, 2012. 55(23-24): p. 7268-7277.
11. Zhou, G. and Z. Feng, Experimental investigations of heat transfer enhancement by plane and curved winglet type vortex generators with punched holes. International Journal of Thermal Sciences, 2014. 78: p. 26-35.
12. Caliskan, S., Experimental investigation of heat transfer in a channel with new winglet-type vortex generators. International Journal of Heat and Mass Transfer, 2014. 78: p. 604-614.
13. Wang, Y., et al., Numerical analysis of flow resistance and heat transfer in a channel with delta winglets under laminar pulsating flow. International Journal of Heat and Mass Transfer, 2015. 82: p. 51-65.
14. Wu, J. and W. Tao, Effect of longitudinal vortex generator on heat transfer in rectangular channels. Applied Thermal Engineering, 2012. 37: p. 67-72.
15. Du, X., et al., Heat transfer enhancement of wavy finned flat tube by punched longitudinal vortex generators. International Journal of Heat and Mass Transfer, 2014. 75: p. 368-380.
16. Gong, B., L.-B. Wang, and Z.-M. Lin, Heat transfer characteristics of a circular tube bank fin heat exchanger with fins punched curve rectangular vortex generators in the wake regions of the tubes. Applied Thermal Engineering, 2015. 75: p. 224-238.
17. Zhou, G. and Q. Ye, Experimental investigations of thermal and flow characteristics of curved trapezoidal winglet type vortex generators. Applied Thermal Engineering, 2012. 37: p. 241-248.
18. Yongsiri, K., et al., Augmented heat transfer in a turbulent channel flow with inclined detached ribs. Case Studies in Thermal Engineering, 2014. 3: p. 1-10.
19. Holman, J.P., Heat transfer. 1986: McGraw Hill.